Numerical analysis of tunable deley-line with an SSB modulator

Tetsuya Kawanishi,
Communications Research Laboratory, Tokyo, Japan

January 6, 2003

Abstract

Recently, we proposed a novel electrically tunable delay-line that has a simple setup [1]. Our system consists of an optical single-sideband (SSB) modulator, a fiber Bragg grating (FBG), and an optical fiber loop. In this report, we investigated the tunable deley-line by using numerical calculations. The principle of the operation is described in the first section. The number of times a lightwave circulates in the loop depends on the frequency of the electric signal applied to the modulator. Thus, we can control the delay by switching the frequency without using delay lines of various lengths. We also discussed the performance of the SSB modulator as an optical frequency shifter, in the second section. A pair of rf-signals having 90 degrees phase difference are applied to the SSB modulator, to obtain the optical frequency shift operation. An electric 90 degrees hybrid coupler is used to generate the rf-signals. However, the phase difference of the coupler has non-negligible deviation from 90 degrees, which causes generation of undesired components in the output of the SSB modulator. We investigated the relations between the signal-to-noise-ratio (SNR) of the output lightwave and the phase deviation of rf-signals fed to the modulator, by using a mathmatical model of the SSB modulator. In the third section, we showed numerical results calculated by *Optisystem 2.2*. The fiber loop consisting of an SSB modulator and an FBG was expressed by a series of modulators and FBGs, in numerical simulations. Although we neglected cross-talk between lightwaves of different wavelengths, numerical results agreed well with experimentally measured data [1].

1 Principle of operation

Our system is comprised of a loop with an optical single-sideband (SSB) modulator. As shown in Fig. 1, the system has an optical port consisting of two optical circulators and an FBG placed between them. A lightwave whose optical frequency is out of the reflection band of the FBG can pass through the port, while a lightwave in the band can not. Thus, an input lightwave whose frequency is out of the reflection band comes into the loop. When the modulator is not in operation, the lightwave goes through the loop once, and then it exits from the port. Consider that the SSB modulator is in operation, and that the input optical frequency (f_0) is slightly lower than the edge of the reflection band, as shown in Fig. 2, where f_m denotes the frequency of the electric signal fed to the modulator, and f_r is the reflection band width of the FBG. The input optical frequency can be shifted at the SSB modulator [2, 3, 4]. We assume that the dc-bias voltages for the modulator are tuned to generate the upper sideband. Of course, we can use the lower sideband instead of the upper sideband when f_0 is slightly higher than the upper edge of the reflection band. The f_0 lightwave, coming into the loop through the port, is input to the SSB modulator, and then its frequency is shifted to the reflection band ($f_0 + f_m$). Thus, the lightwave is reflected by the FBG, and circulates in the loop again. During the successive circulation steps, the optical frequency is shifted at the modulator. After n times circulation, the frequency of the lightwave becomes $f_0 + nf_m$. We call such a spectral component an n-th order channel. After circulating several times, the lightwave exits the reflection band, where the number of circulation steps p is given by $pf_m > f_r > (p-1)f_m$. In this paper, we call the spectral component of $f_0 + pf_m$ the prime channel, which is the lowest order channel in the channels whose frequency is higher than the reflection band. The output lightwave contains some other components resulting from the nonlinearlity of the modulator and residual transmittance in the reflection band. However, the prime channel would be dominant when we can consider that f_m is larger than the edge slope width of the reflection band, and that any high-order harmonic generation at the modulator is negligible. The propagation delay of a circulation step is given by $\tau = l/c$, where l denotes the effective optical length of the loop, and c is the speed of light. The delay of the prime channel at the loop is dependent on f_m, as follows: $p\tau = \tau \times Int(f_r/f_m)$, where $Int(x)$ gives the smallest integer larger than x. Thus, we can change the delay $p\tau$ by switching the frequency of the electric signal f_m. The frequency can

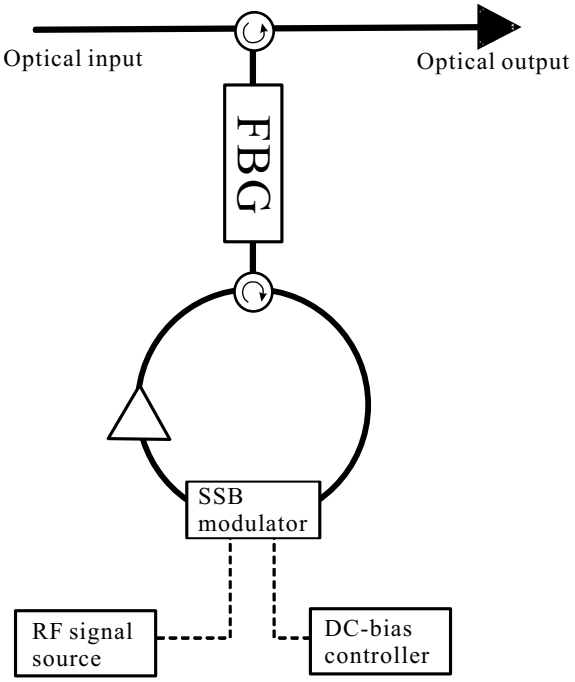

Figure 1: Tunable delay-line with optical frequency shift

be switched at any time except when a packet is passing the SSB modulator, thus it is not necessary to synchronize the switching timing with the propagation cycle of the packet. In addition, we note that pulses longer than the optical length l can pass the delay loop without any collisions owing to frequency shift at the modulator.

2 Optical SSB modulator

The SSB modulator consists of parallel four optical phase modulators as shown in Fig.3. The electric field of the output lightwave can be expressed by

$$E = \frac{\mathrm{e}^{\mathrm{i}2\pi f_0 t}}{4} \times \sum_{n=-\infty}^{\infty} \mathrm{e}^{\mathrm{i}n2\pi f_m t} \sum_{j=1}^{4} J_n(A_j^{\mathrm{RF}}) P_{n,j} A_j^{\mathrm{LW}}, \tag{1}$$

where

$$P_{n,j} \equiv \exp \mathrm{i} \left[(1 - Sn) j \frac{\pi}{2} + \Delta\phi_j^{\mathrm{LW}} + n\Delta\phi_j^{\mathrm{RF}} \right] \tag{2}$$

$$\phi_j^{\mathrm{LW}} = \frac{j\pi}{2} + \Delta\phi_j^{\mathrm{LW}} \tag{3}$$

$$\phi_j^{\mathrm{RF}} = -S\frac{j\pi}{2} + \Delta\phi_j^{\mathrm{RF}} \tag{4}$$

$$S = \pm 1. \tag{5}$$

J_n expresses the first kind n-th order Bessel's function. ϕ_j^{RF} and ϕ_j^{LW} denote the phases of rf-signal and lightwave in Path j. $\Delta\phi_j^{\mathrm{RF}}$ and $\Delta\phi_j^{\mathrm{LW}}$ are the deviations of the phases from the ideal condition for the SSB modulation. A_j^{RF} and A_j^{LW} denote the amplitudes of rf-signal and lightwave in Path j. When $\Delta\phi_j^{\mathrm{RF}} = \Delta\phi_j^{\mathrm{LW}} = 0$, the phases are 0, 90, 180 and 270 degrees. The SSB modulator has a pair of Mach-Zehnder structures, so that we can apply

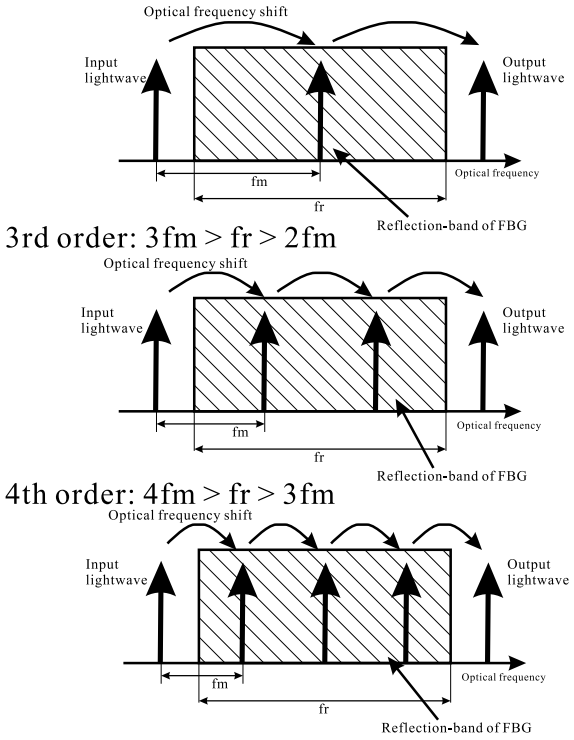

Figure 2: Principle of the operation

rf-signals of 0, 90, 180 and 270 degrees by feeding a pair of rf-signals with 90 degrees phase difference at two rf-ports ($\mathrm{RF_A}$, $\mathrm{RF_B}$). The rf-signals can be obtained by using rf 90 degrees hybrid coupler. The optical phase differences are set to be 90 degrees, by using dc-bias ports ($\mathrm{DC_A}, \mathrm{DC_A}, \mathrm{DC_A}$). When the intensity of the rf-signal is so small that we can neglect high-order harmonic generation at the optical phase modulation, the output optical spectrum defined by Eq. (1) for $S = 1$ can be approximately expressed by

$$E \simeq A^{\mathrm{LW}} \mathrm{e}^{\mathrm{i}2\pi f_0 t} \left[J_1(A^{\mathrm{RF}}) \mathrm{e}^{\mathrm{i}2\pi f_m t} - J_3(A^{\mathrm{RF}}) \mathrm{e}^{-\mathrm{i}3\times 2\pi f_m t} \right], \tag{6}$$

where A^{RF} denotes the amplitude of the rf-signal, which corresponds to the optical induced phase at each modulator. Because $J_1 > J_3$, the dominant component in the output is the first order upper sideband, which corresponds to the frequency shifted component. On the other hand, in the case of $S = -1$, the lower sideband can be obtained instead of the upper sideband. We can easily switch the polarity of S, by changing the dc-bias voltage applied on the port $\mathrm{DC_C}$. The SNR and conversion efficiency of the frequency shift by the modulator are given by $J_1(A^{\mathrm{RF}})/J_3(A^{\mathrm{RF}})$ and $J_1(A^{\mathrm{RF}})$, respectively. In actual setups, $\Delta\phi_j^{\mathrm{RF}}, \Delta\phi_j^{\mathrm{LW}} \neq 0$, so that the SNR is less than the theoretical limit given by J_1/J_3. The phase errors of the rf-signal due to the hybrid coupler is dominant in generation of undesired spectra components. However, as shown in Eq.(2), $\Delta\phi^{\mathrm{RF}}$ can be compensated by $\Delta\phi^{\mathrm{LW}}$. Fig. 4 shows the SNRs as functions of the phase error at the hybrid coupler. We get high SNR even when $\Delta\phi^{\mathrm{RF}}$ is large by using the compensation of the phase error. The amplitudes of rf-signals and lightwaves were assumed to be balanced in this numerical calculation. We can control the phases of lightwaves by using dc-bias ports. The phase error at the hybrid can be compensated easily and agilely by tuning dc-voltage sources.

3 Numerical results

We investigated the tunable delay-line by using a lightwave network simulator, *OptiSystem 2.2*, where we define optical input and output ports in each component. As shown in Fig. 1, the lightwave propagates several times in the loop, but the lightwave can get into the port only once in this simulator. By neglecting cross-talks between channels

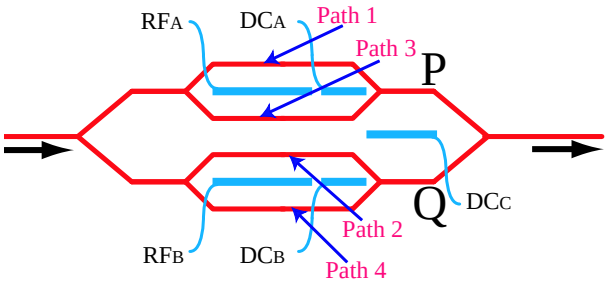

Figure 3: Optical SSB modulator

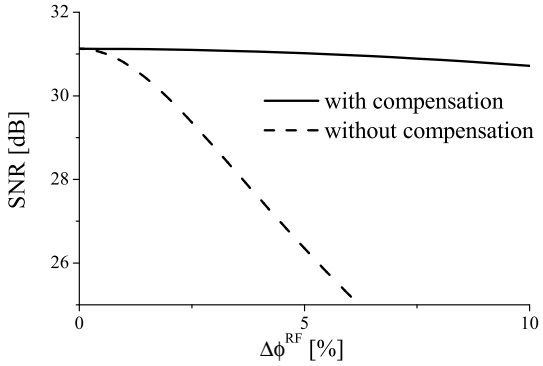

Figure 4: SNR of output from SSB modulator for $A^{\mathrm{RF}} = 0.8$rad.

at the optical amplifier, the delay-line can be expressed by a model described in Fig. 5, where the lightwave comes into each port only once. The successive circulation steps in the loop is expressed by a series of loop units, where the model of the loop unit consists of an optical amplifier, an FBG, and an optical SSB modulator, as shown in Fig. 6. The SSB modulator was described by four optical phase modulators. By using the models defined by Figs. 5 and 6, we numerically calucalated time domain profiles and spectra of output lightwave of the tunable delay-line. Input lightwave power and frequency were set to be 10 dBm and 193.37 THz. The gain and noise figure of the optical amplifier were, respectively, 16 dB and 6 dB. The delay (τ) and attenuation in the loop were 350 ns and 10 dB. FBGs were assumed to be uniform gratings whose center frequency and bandwidth were, respectively, 193.388 THz and 33 GHz. We also put an FBG at the output of the model defined in Fig. 6, in order to eliminate the input lightwave component reflected at the FBG in the loop unit. Figs. 7 and 8 show the frequency domain spectra and the time domain envelopes of the output lightwaves, where the induced phase at each optical phase modulator in the SSB modulator (A^{RF}) was 1.22. The rf frequencies for 2nd, 3rd and 4th channels, were, respectively, 18, 12 and 9 GHz. The input lightwave was intensity modulated by a train of pulses whose width was 800 ns. As shown in Fig. 8, the delay can be controlled by changing the frequency of the electric signal fed to the SSB modulator. The delay due to one step of the circulation (τ) corresponding to the time difference between adjoining channels, was 350 ns, while the pulse width is 800 ns. Eye diagrams of the output lightwave were shown in Figs. 9 and 10, where the input lightwave was intensity modulated by a 2.5 Gbit/s NRZ signal. The devitaions of zero and mark levels were larger in the higher order channel (see the 4th channel), especially in the case of $A^{\mathrm{RF}} = 1.22$. We deduce that this is due to the interference between adjecent channels. The ratio of the undesired components to the desired one was larger when the order of the cannel (p) was high, as shown in Fig. 7.

We also calculated Q-factors as functions of the induced phase A^{RF}. The frequency conversion efficiency at the SSB modulator is given by $J_1(A^{\mathrm{RF}})$, so that the intensity of the desired component is an increasing function of A^{RF} when $A^{\mathrm{RF}} < \pi/2$. On the other hand, when A^{RF} is large, the SNR of the lightwave is significantly decreased by the third order harmonics generated at the SSB modulator, as shown in Eq. (6). Due to this trade-off relations, Q-factors had maxima as shown in Fig. 11. The Q-factor for 2nd channel had a peak at $A^{\mathrm{RF}} \simeq 1.0$. For 3rd and

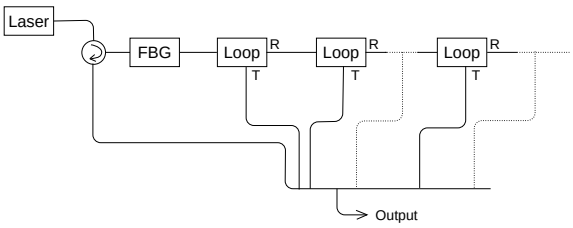

Figure 5: Model of proposed delay-line used in numerical calculation

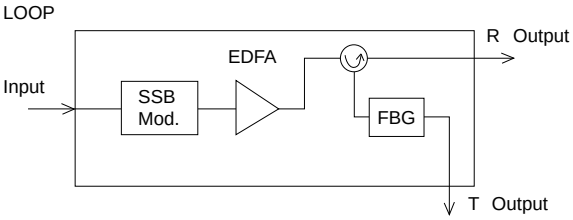

Figure 6: Model of the loop unit

4th channels, there were maxima at $A^{\mathrm{RF}} \simeq 1.6$ and 2.0, respectively. The optimal induced phase depends on the number of the circulation steps p.

References

[1] T. Kawanishi, S. Oikawa, K. Higuma and M. Izutsu, Electrically Tunable Delay-line using an Optical Single-Sideband Modulators, *IEEE Photon. Tech. Lett.*, Vol. 14, 1454-1456 (2002)

[2] S. Shimotsu, S. Oikawa, T. Saitou, N. Mitsugi, K. Kubodera, T. Kawanishi, and M. Izutsu, "LiNbO3 Optical Single-Sideband Modulator," OFC 2000, PD-16

[3] S. Shimotsu, S. Oikawa, T. Saitou, N. Mitsugi, K. Kubodera, T. Kawanishi, and M. Izutsu, "Single Side-Band Modulation Performance of a LiNbO3 Integrated Modulator Consisting of Four-Phase Modulator Waveguides," *IEEE Photon. Tech. Lett.*, Vol. 13, 364-366 (2001)

[4] S. Shimotsu, M. Izutsu, T. Kawanishi, S. Oikawa, and M. Sasaki, "Wideband Frequency conversion with LiNbO3 optical single-sideband modulator," OFC 2001, WK3-1

[5] K. Higuma, S. Oikawa, Y. Hashimoto, H. Nagata, and M. Izutsu, "X-cut lithium niobate optical single-sideband modulator," *Electron. Lett.*, Vol. 37, 515-516 (2001)

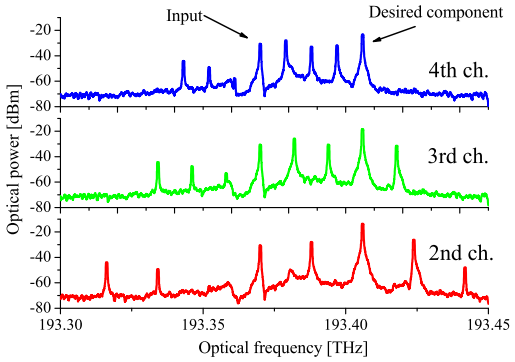

Figure 7: Optical spectra of the output lightwave for $A^{\mathrm{RF}} = 1.22$.

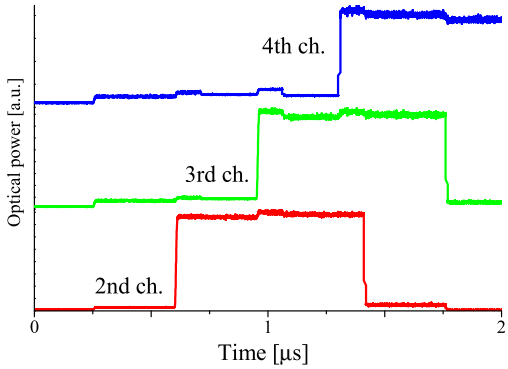

Figure 8: Time domain envelopes of the output lightwave for $A^{\mathrm{RF}} = 1.22$.

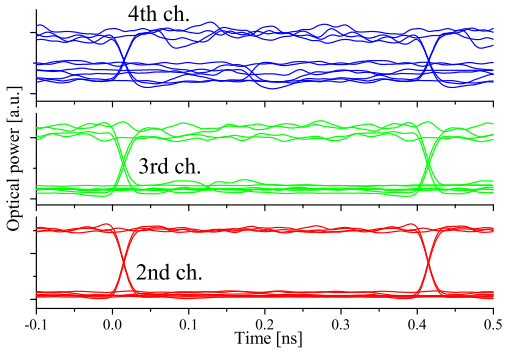

Figure 9: Eye diagram of output lightwaves, where A^{RF}=1.22.

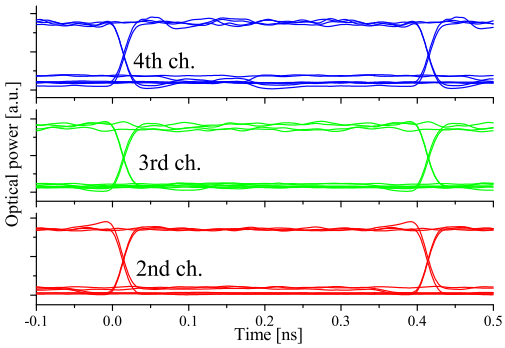

Figure 10: Eye diagram of output lightwaves, where A^{RF}=1.57.

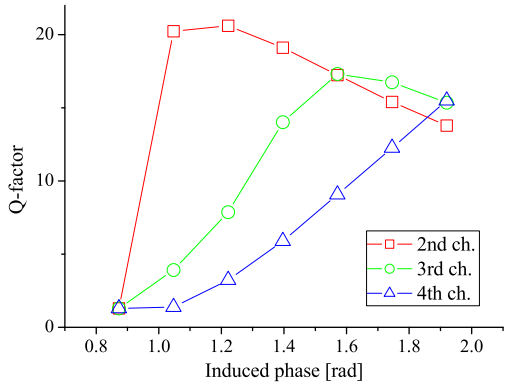

Figure 11: Q-factors of output lightwaves as functions of induced phase A^{RF}.